

GRAVITY MODELING OF SUBSURFACE STRUCTURES AND RESERVOIR CHARACTERIZATION USING SEISMIC INVERSION IN THE NIAS BASIN

PEMODELAN GAYABERAT STRUKTUR BAWAH PERMUKAAN DAN KARAKTERISASI RESERVOIR MENGGUNAKAN INVERSI SEISMIK DI CEKUNGAN NIAS

Ramadhana Wibowo^{1,3*}, Imam Setiadi², Yulinar Firdaus², Riza Rahardiawan²

¹Departement of Geophysical Engineering, Institut Teknologi Sepuluh Nopember, Surabaya

²Marine Geological Institute, Bandung

³Pertamina Hulu Mahakam, Balikpapan

*Corresponding author: ramadhana.wibowo@gmail.com

(Received 15 June 2024; in revised from 23 August 2024 accepted 27 November 2024)

DOI : 10.32693/bomg.39.2.2024.890

ABSTRACT: The development of interpretation techniques opens new exploration opportunities in the forearc basins of western Indonesia, such as the Nias Basin which show signs of oil and gas seepage. Gravity and seismic inversion analysis were used to look into the Nias Basin in order to evaluate its subsurface structure, the location of sedimentary sub-basins, and the possible presence of hydrocarbon reservoirs. After filtering the data for the Complete Bouguer Anomaly (CBA), a residual anomaly was obtained. This allowed for the quantitative interpretation of structures below the surface using 2D gravity forward modelling. Seismic and well data interpretation includes sensitivity analysis, a well-seismic tie, picking horizons, and acoustic impedance (AI) inversion. The residual gravity anomaly reveals eight sub-basin patterns spread out in the Nias Basin with a relative continuity direction of northwest-southeast following the lineaments of basement highs. The subsurface geological model identified four rock formations. From deepest to shallowest, these units are metamorphic bedrock (2.7 g/cc), Lelematua Formation (2.5 g/cc), Gomo Formation (2.4 g/cc), and Gunungsitoli Formation with an overlying alluvium (2.25 g/cc). Interpretation of well and seismic suggests a target zone at a 2,017 – 2,101 meters depth. Using a model-based hard constraint for AI inversion in this zone indicates possible carbonate reservoirs. Based on sensitivity analysis with an interval of 34,000 - 47,000 (ft/s)*(g/cc), an AI cutoff value of more than 34,000 (ft/s)*(g/cc) was obtained. The carbonate is estimated to be a tight carbonate in the limestone of the Gomo Formation.

Keywords: CBA, 2D gravity forward modeling, AI inversion, tight carbonate, Nias Basin

ABSTRAK: Perkembangan teknik interpretasi membuka peluang eksplorasi baru di cekungan busur muka bagian barat Indonesia, seperti di Cekungan Nias yang menunjukkan adanya rembesan minyak dan gas. Analisis gaya berat dan inversi seismik digunakan dalam kajian Cekungan Nias untuk evaluasi struktur bawah permukaan, lokasi sub-cekungan sedimen, dan kemungkinan adanya reservoir hidrokarbon. Proses penapisan dilakukan terhadap data Complete Bouguer Anomaly (CBA) untuk memperoleh anomali residual. Anomali ini digunakan dalam interpretasi kuantitatif struktur bawah permukaan melalui pemodelan kedepan 2D data gayaberat. Interpretasi data seismik dan sumuran meliputi analisis sensitivitas, well seismic tie, picking horizon serta inversi acoustic impedance (AI). Anomali residual menunjukkan delapan sub-cekungan sedimen yang tersebar pada area Cekungan Nias dengan arah kemenerusan relatif

barat laut – tenggara mengikuti pola kelurusan tinggian. Empat formasi batuan diidentifikasi dari hasil pemodelan geologi bawah permukaan. Urutan satuan paling dalam hingga teratas adalah batuan dasar metamorf (2,7 g/cc), Formasi Lelematua (2,5 g/cc), Formasi Gomo (2,4 g/cc), dan Formasi Gunungsitoli dengan alluvium di atasnya (2,25 g/cc). Interpretasi sumur dan seismik menunjukkan zona target pada kedalaman 2.017 – 2.101 meter. Dengan menggunakan model berbasis hard constraint untuk inversi AI pada zona ini menunjukkan kemungkinan keberadaan reservoir karbonat. Berdasarkan analisis sensitivitas dengan interval 34.000 - 47.000 (ft/s)*(g/cc), diperoleh nilai batas AI lebih dari 34.000 (ft/s)*(g/cc). Karbonat tersebut diperkirakan merupakan tight carbonate pada batugamping Formasi Gomo.

Kata Kunci: CBA, pemodelan kedepan 2D gayaberat, inversi AI, tight carbonate, Cekungan Nias

INTRODUCTION

Driven by the need for new hydrocarbon sources, exploration efforts are increasingly turning towards re-evaluating sedimentary basins with potential reserves, previously overlooked in forearc basins such as the Nias Basin. At the same time, historical drilling results in the Nias Basin suggested limited hydrocarbon prospects; Union Oil has discovered oil and gas seeps in Nias waters and drilled a few wells there (Rose, 1983). Based on this new evidence, a significant re-evaluation of the hydrocarbon potential of the Nias Basin is needed (Sapiie, 2015). Geological features revealed by recent seismic data indicate promising prospects for future exploration (Deighton et al., 2014). Therefore, further comprehensive geological and geophysical investigations are required to describe the extent and sustainability of potential resource in the Nias Basin.

This study proposes an integrated geophysical approach to assess the hydrocarbon potential of the Nias Basin, including gravity and seismic inversion methods. Gravity analysis differentiates the density of an anomalous source from the surrounding environment, providing insight into the description of subsurface geological structures through density variations (Setiadi et al., 2014). Previous gravity analysis studies have succeeded in delineating sedimentary sub-basins, revealing structures and faults in the Akimeugah Basin (Setiadi, et al., 2019), and identifying hydrocarbon prospect structures in other basins (Erviantari & Sarkowi, 2014; Dewi, et al., 2020). By integrating gravity data with geological and others geophysical information, we can estimate the thickness and depth of sedimentary sequences, identify fault systems and basement structures (Lghoul et al., 2023, Saada et al., 2022; and El-Sehamy et al., 2022;). Seismic inversion has been used in oil and gas exploration for reservoir characterization (Pradana et al., 2017). This method improves information on subsurface lithology in sedimentary basins. Studies by Alifudin et al. (2016)

showed the presence of bright spots on seismic sections as indicators of high porosity zones and hydrocarbon prospects. Acoustic impedance (AI) inversion modeling has been successful in delineating zones with high AI values, which were identified as carbonate rock reservoirs.

This study combines gravity analysis, seismic inversion, and geological setting to provide a comprehensive subsurface image, patterns of sediment distribution in the sub-basin, and indications of hydrocarbon potential in the Nias Basin and its surroundings.

Geological Setting

Located in the northwestern part of Sumatra, the Nias Basin extends northwest-southeast between the Sunda Arc subduction zone and the Sumatra Fault (Figure 1). This Tertiary basin covers land and offshore areas to the east of Nias Island. It is estimated at 10.880 km², with most of 9.153 km² in the waters east of Nias Island and the remaining 1.727 km² on the island itself. The Nias Basin is traversed by several major faults, including the Batee and Mentawai Faults (Karig et al., 1980). These structures formed due to oblique subduction of the northward-moving Indo-Australian Plate beneath the Eurasian Plate. The subduction event that occurred in the Late Eocene to Early Oligocene triggered the formation of the Sumatran Fore-Arc, followed by the Sunda Trench in the Late Oligocene. The formation of this fore-arc began with the opening of the Fore-Arc Basin, typically marked by the formation of trench sedimentary folds that coincided with the Sunda Trench during the Oligocene to Early Miocene (Permana et al., 2010).

Various rock formations record the layered geological history of the Nias Basin. The youngest layer is the Alluvium Formation, a thin 2-5 m Holocene deposit consisting of river, swamp and coastal sediments such as limestone blocks, sand, silt and clay. Below this lies the Gunungsitoli Formation,

reaching 120 m in thickness. Deposited during the Pliocene-Pleistocene, the formation is rich in various limestones (reef, lagoonal, and calcareous), marl, and sandy clay. These limestones are primary reservoir targets due to their ability to store hydrocarbons.

At greater depths lies the Gomo Formation, a thicker layer (1250-2500 m) deposited from the Middle Miocene to Early Pliocene. This formation is a complex assemblage of mudstone, marl, sandstone, and limestone, with interbeds of tuffaceous marl, tuff, and even peat. Similar to the Gunungsitoli Formation, some Gomo Formation limestones have potential as hydrocarbon reservoirs. The Lelematua Formation, another thick layer (up to 3000 m) deposited during the Early to Late Miocene, follows the Gomo Formation. Characterized by alternating layers of sandstone, mudstone, siltstone, conglomerate, and tuff, the Lelematua Formation occasionally contains thin coal seams and shale. Specific interbeds of sandstone from the Early Miocene within this formation could serve as reservoir rocks. The deepest layer is the Bancuh Complex, a heterogeneous mixture of various rock types formed during the Early Oligocene to Early Miocene. This complex includes peridotite,

serpentinized gabbro, serpentinite, basalt, schist, shale, graywacke, conglomerate, breccia, limestone, sandstone, and chert.

METHODS

Gravity Analysis

The Complete Bouguer Anomaly (CBA) data used in this study was obtained from the Marine Geological Institute (MGI) (Rahardiawan, 2018). The data underwent spectral analysis to estimate the anomaly depth and determine the window width for separating anomalies. High-pass and low-pass filters separated the data into regional and residual anomalies. Through the application of these filters on potential field data, their remarkable efficiency and precision in qualitatively delineating and interpreting geological structures have been demonstrated (Nzeuga et al., 2022; Pham et al., 2023). The residual anomaly was then qualitatively interpreted to identify basin highs and sub-basin patterns in the Nias Basin. Various reference parameters were considered in model creation, including depth values from spectral analysis, fault location and type from derivative analysis, and stratigraphic information.

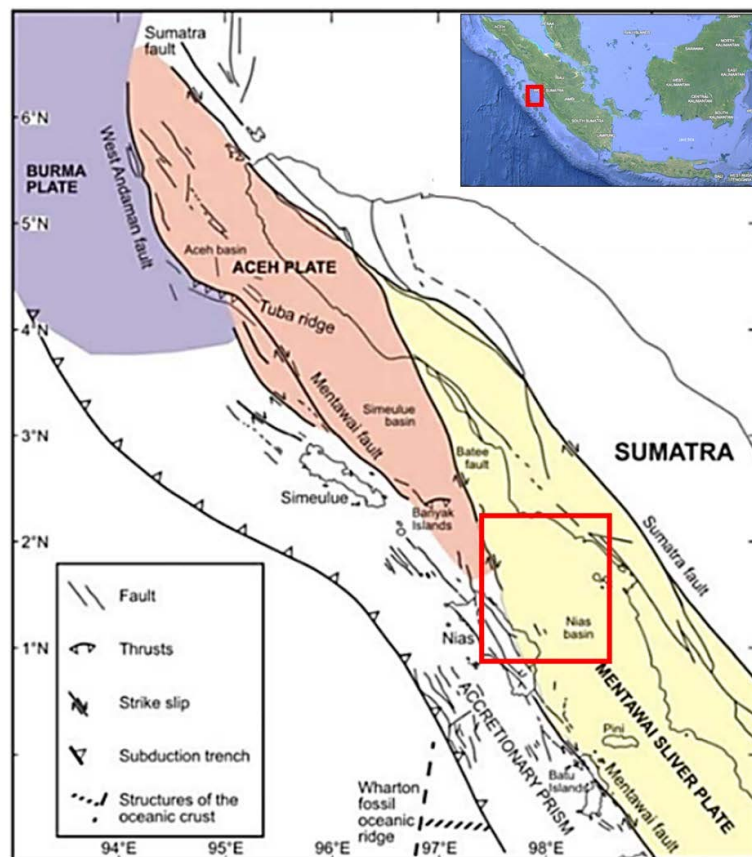


Figure 1. Study area (red square) and tectonic elements of the Nias Basin (Karig et al., 1980)

Iterative trial-and-error improved the model response curve until it closely matched the observed gravity data curve. It reduced the difference between the modelled and actual subsurface conditions as much as possible (Talwani, 1959).

It is important to note that while gravity analysis provides a broad and regional perspective on subsurface structures, its resolution is inherently less detailed compared to seismic methods. Therefore, seismic inversion, particularly when supplemented with borehole data, offers a more precise delineation of subsurface features, enhancing the overall interpretation (Telford et al., 1990).

Seismic inversion

Seismic inversion turns seismic reflection data into numerical descriptions of geology and lithology, using borehole data as a guide to figure out the properties of rocks below the surface (Prastika et al., 2018). The outcome of seismic inversion is extracting acoustic impedance information embedded within the rock layers. This information is crucial for characterizing reservoir properties such as porosity and fluid content.

Pusdatin ESDM owns the data used in this research. Seismic processing begins with a well seismic tie, which correlates the laterally well-resolved seismic data and the vertically high-resolution well data. This process ensures maximum data validity. Following well tie, horizon picking is conducted by making horizon lines representing layer continuity within the seismic section. The picking horizon defines the upper and lower boundary of the target zone. Subsequently, the seismic inversion process, which includes creating an

initial model, utilizes several sequences within the seismic section. One can generate subsurface physical properties through inversion modeling, particularly acoustic impedance (AI) values. The seismic section produced as a result illustrates the subsurface geological model. To enhance the accuracy of the seismic inversion results, the calibration of the inversion models with well data was carefully conducted, and multiple iterations were performed to minimize discrepancies. This approach ensures that the subsurface physical properties inferred from the inversion process closely represent the actual geological conditions.

RESULTS

Gravity Analysis

The Complete Bouguer Anomaly (CBA) illustrates the distribution of gravity differences and density variations resulting from different rock types beneath the Earth's surface. Processing field data and making various adjustments, including corrections for tidal fluctuations, latitude differences, the Eötvös effect, terrain, and the Bouguer correction, leads to the calculation of the CBA value. Examination of the CBA map for the research area identifies three distinct subsurface regions (Figure 2). A region with high anomalies (53-76 mGal) in the south, northeast, and southwest indicates the presence of uplifted structures or dense basement rocks. Moving towards the east, a region with moderate anomalies (42-52 mGal) spanning the southeast, central, and northwestern areas signifies transitional rocks. Additionally, a region with low anomalies (-18 to 41 mGal) in the northwest is associated with low-density sedimentary rocks that fill sub-basins.

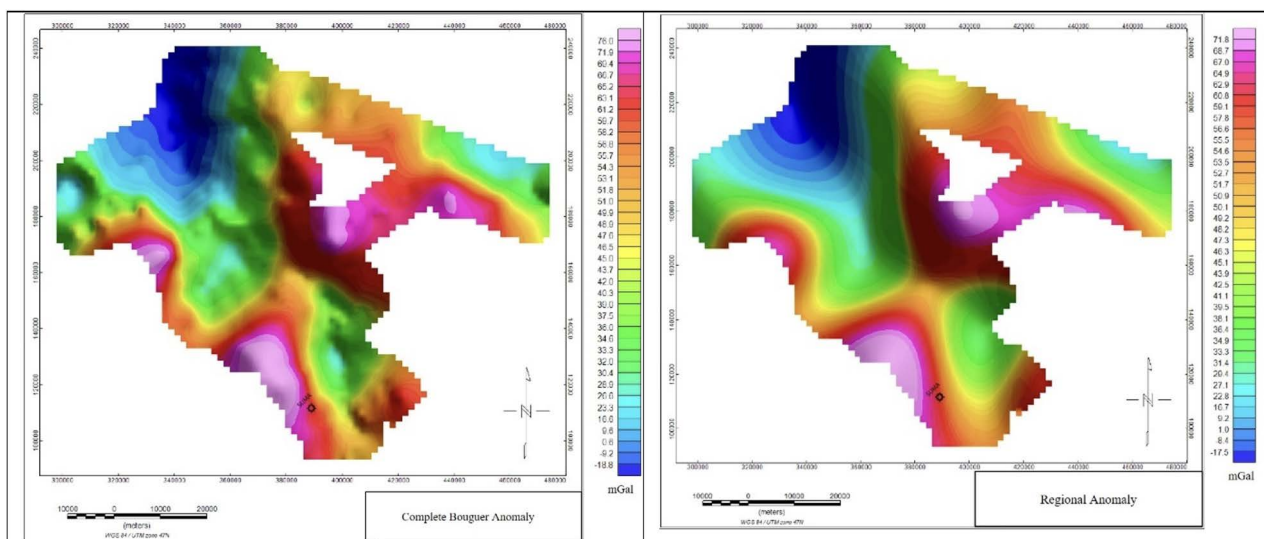


Figure 2. CBA and regional anomaly in Nias Basin

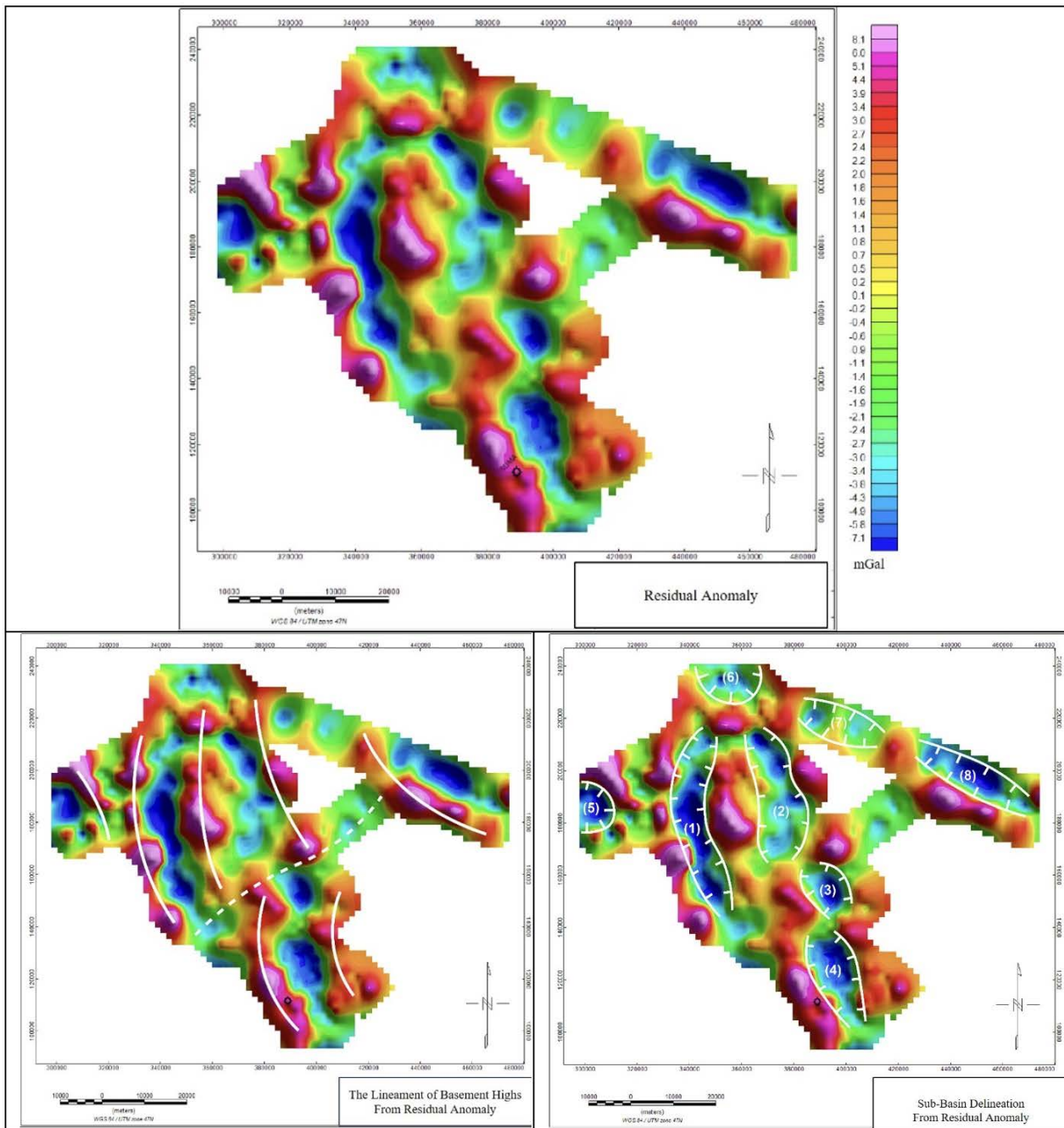


Figure 3. Residual anomaly, the lineament of basement highs and sub-basin delineation of Nias Basin

The Complete Bouguer Anomaly (CBA) combines two anomaly components: regional anomalies from deeper sources and residual anomalies caused by shallower sources. Separating these regional and residual anomalies from the CBA enables a clearer understanding of the bedrock and subsurface structures. Techniques such as spectral analysis and filtering separate these anomaly components, allowing for a detailed look at the region's geological features.

Spectral analysis shows that the regional zone lies at an average depth of 13.5 km and is thought to

be the boundary depth between the upper and lower crust. The average depth of the residual zone is estimated to be 2.8 km, corresponding to the depth of the boundary between the sedimentary layer and the basement rock. These findings are consistent with the regional geological map of the Nias sheet (Djamel et al., 1994), which indicates a sedimentary thickness of approximately 2-4 km in the Nias area.

The regional anomaly is derived from applying a low-pass filter with a cutoff wavelength of 40 km, a value obtained from the spectral analysis of the CBA. Figure 2 illustrates two different patterns of regional

anomalies: a high anomaly (52-71 mGal) located in the southern, southwestern, and northwestern regions, interpreted as a response to uplifted basement rocks; and a low anomaly (-17-39 mGal) centered in the northwestern region, which is assumed to result from basement rocks that have been displaced downwards.

Furthermore, the residual anomaly of the Nias Basin, obtained by applying a high-pass filter with a cutoff wavelength of 40 km, originates from shallow

sources with high frequency and short wavelength. It creates a more complex contour pattern compared to the CBA anomaly. Both high and low anomalies are present in the residual anomaly pattern in the study area (Figure 3). Red-pink zones on the map signify high anomalies, suggesting basement highs resulting from the uplift of bedrock with a higher density contrast than the surrounding areas. Basement high structures mark the boundaries between different sub-basins. Low anomaly zones characterized by

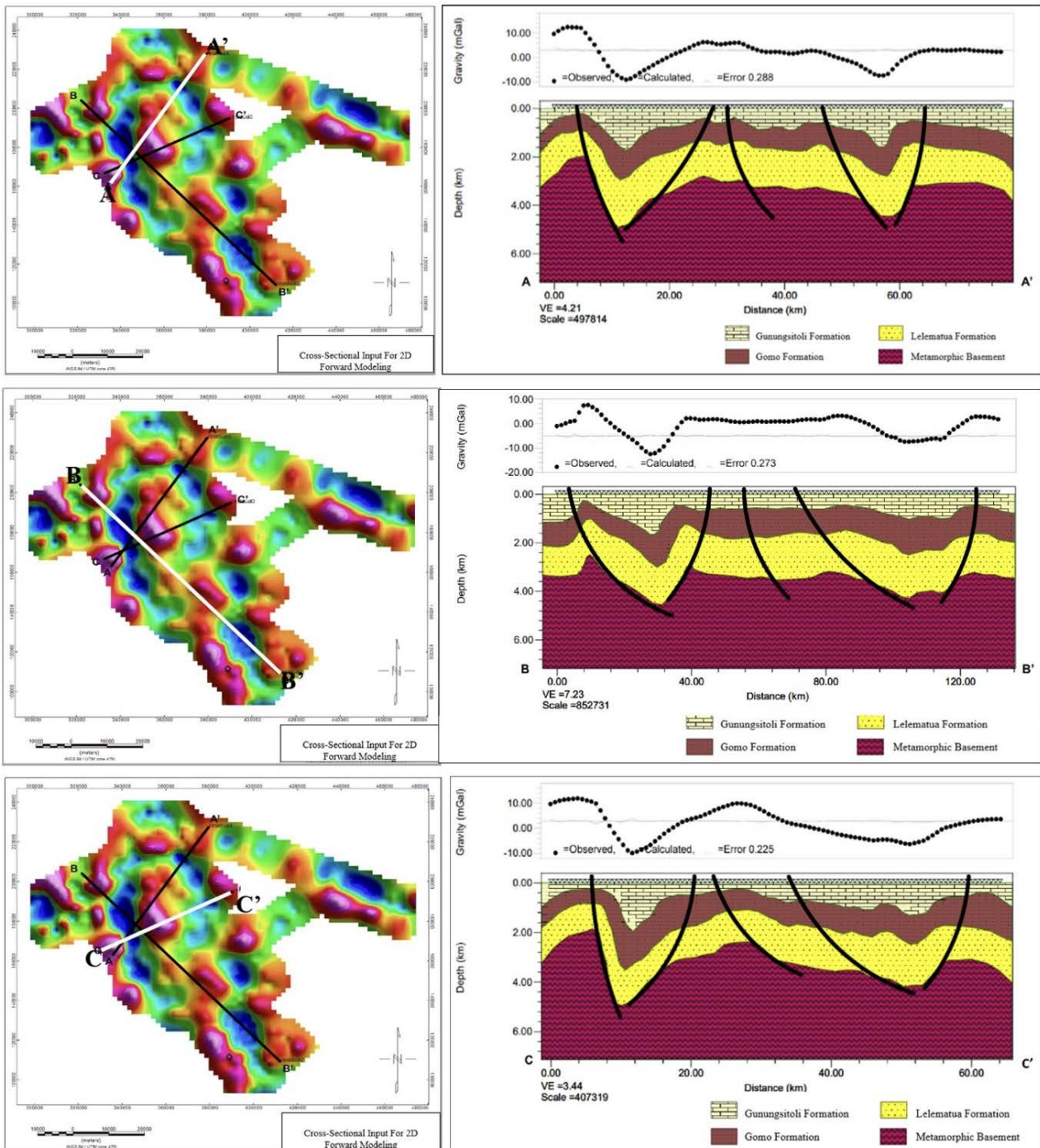


Figure 4. Cross-sectional 2D model of AA', BB', and CC'

blue-green colours are suspected to be sedimentary sub-basins with low density contrast.

Based on the analysis of the residual anomaly, the basement highs and sub-basins were delineated. Figure 3 shows lineament of basement highs with a general northwest-southeast trend. The Indian Ocean crust subducting perpendicular to the Nias Basin lineament is most likely the cause of it.

Analysing the basement high lineament has helped delineate eight sub-basins within the Nias Basin. These sub-basins may have formed due to the movement of the Earth's crust, possibly caused by the Indian Ocean plate sliding beneath. Sub-basin 1, located north of Nias Island, has a distinct geophysical signature with a deep blue colour, indicating that it may have a much thicker layer of sediments than the other sub-basins. Given the regional geological layout, the fact that there is an elevated area to the east of sub-basin 1 suggests that there could be conditions that are advantageous for gathering oil and gas. A detailed analysis using seismic methods and exploratory drilling in this area is recommended to validate this possibility.

A quantitative analysis of residual anomaly from the Nias Basin was conducted using a 2D forward modeling approach. This method provides detailed information about the subsurface, including layer thickness, lithology, basement depth, and geological structure. The depth to basement obtained from spectral analysis was used as the main reference for the model construction.

In Figure 4, the modeling was performed along the southwest-northeast direction cross-section of AA'. The initial model was constructed based on stratigraphic information and rock density data. The high-density anomaly in the central part of the cross-

section is probably caused by metamorphic basement rocks comprising various rock types, including peridotite, gabbro, serpentinite, basalt, and schist, which were relatively uplifted. The low-density anomalies on the left and right sides of the cross-section suggests the presence of sedimentary basins.

The subsurface model of AA' consists of four rock formations. The bottommost layer is interpreted as the metamorphic basement rock underlying the basin, with a density value of 2.7 g/cc. The 2.5 g/cc Lelematua Formation overlies the basement, consisting of sandstone, interbedded mudstone and siltstone, conglomerate, and tuff. The next overlying layer is assumed to be the Gomo Formation, comprising mudstone, shale, intercalations of sandstone and limestone, tuff, and peat, with a rock density of 2.4 g/cc. The topmost layer is interpreted as the Gunungsitoli Formation and the alluvium, having a density of 2.25 g/cc. Based on stratigraphic information, the Gunungsitoli Formation is composed of reef limestone, marly limestone, and calcareous sandstone, as well as alluvium containing river, swamp, and coastal deposits consisting of limestone boulders, sand, silt, and clay.

The variation in sediment thickness along AA' (2.8-4 km) suggests a sub-basin. The black line encloses a depocenter formed by subsidence, bounded by surrounding highs. Two depocenters are identified in the western and eastern parts of the cross-section.

Intersecting AA', cross-section BB' is created diagonally from northwest to southeast. The thickness of layers along BB' range from 3.1 km to 4.2 km, with thicker deposits concentrated in the western and eastern flanks. These thicker sequences represent a sub-basin depocenter bounded by surrounding highs.

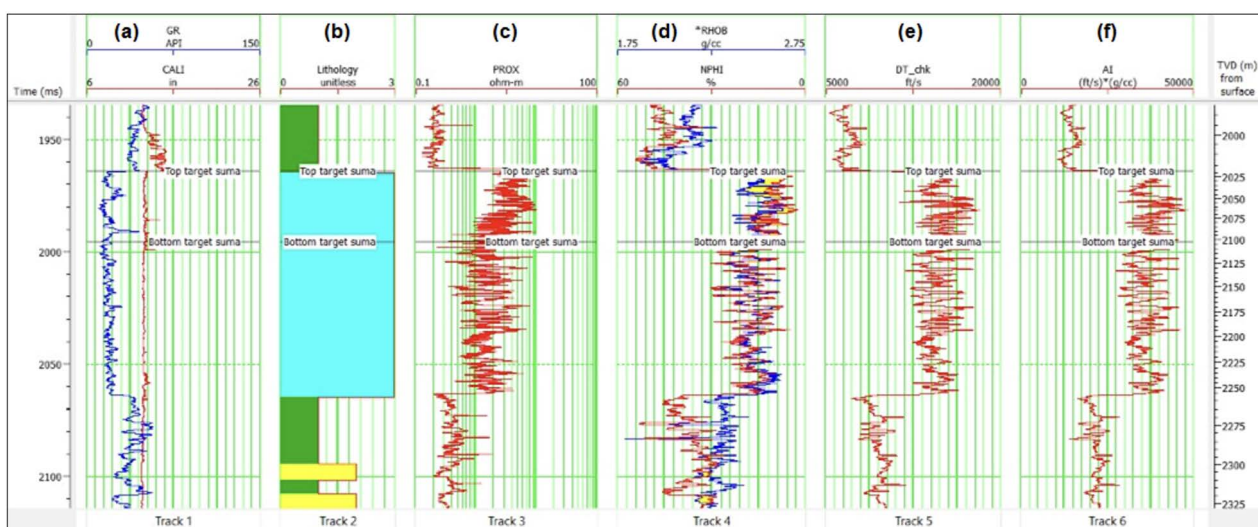


Figure 5. Target zone of Suma-1

A third cross-section, CC', is nearly parallel to AA' (southwest-northeast) and intersects BB'. The modeled rock layers in CC' reveal a sediment thickness variation between 2.6 km and 4.1 km. Structure of CC' exhibits a structural resemblance to AA' due to the near-identical orientations of both cross-sections.

Seismic inversion

A target zone analysis

Qualitative analysis of Suma-1 well logs (Figure 5) including (a) Gamma Ray, (b) lithology, (c) resistivity, (d) RHOB and NPFI, (e) P-wave, and (f) calculated AI; identified a potential reservoir target zone at approximately 2017 to 2101 m. The Gamma Ray log (Figure 5a) is widely used for determining potential lithology and estimating shale content. It determines the type of rock formations in the wells within the research area based on the measured API value. High Gamma Ray values (> 75 API) indicate a high content of shale and clay in the rock, which are classified as non-reservoir rocks due to their low porosity and permeability. Low Gamma Ray values (< 75 API) indicate sandstone and limestone lithology with low shale content, suggesting potential reservoir rocks with high porosity and permeability. The Gamma Ray log shows a leftward deflection with low values of 14 to 30 API at depths ranging from 2017 to 2101 m.

Based on these values, this depth range is interpreted as a potential limestone reservoir zone. The lithology log (Figure 5b) supports this interpretation, indicating limestone in the target zone and mudstone above it. Resistivity log analysis (Fig. 5c) can distinguish between reservoir and non-

reservoir layers by determining the type of fluid content. It is commonly used to detect the presence of porous and permeable rocks containing hydrocarbon or water fluids. The resistivity log can provide information on the resistivity values in the well and estimate the type of fluid content in the rock. Layers containing water have a resistivity curve with a leftward deflection, indicating a low resistivity value due to the water's conductive nature. Layers containing hydrocarbon fluids (oil or gas) will exhibit a rightward deflection of the resistivity curve or a high resistivity value. The reservoir target zone in the research well is located at a depth of 2017 to 2101 m and is suspected of containing oil or gas, as evidenced by a resistivity curve that deflects to the right.

The characteristics of reservoir target zones are typically assessed using neutron porosity (NPFI) and density porosity (RHOB) logs (Figure 5d). The NPFI and RHOB log curves are usually shown in the same column. A crossover between the curves of these two logs indicates the presence of fluid in a layer. These two logs are correlated to determine the type of fluid present in a reservoir zone, specifically gas, oil, and water, as well as the fluid contact boundary. Reservoir zones filled with gas will show a larger crossover between the NPFI and RHOB log curves compared to oil-filled reservoir zones. Oil-filled reservoir zones will have a smaller crossover than gas-filled reservoir zones. Water-filled reservoir zones will have little to no crossover between the NPFI and RHOB log curves. The Suma-1 well reservoir target zone, at a depth of 2017-2101 m, shows a crossover of the NPFI and RHOB log curves, as indicated by the yellow zone. This

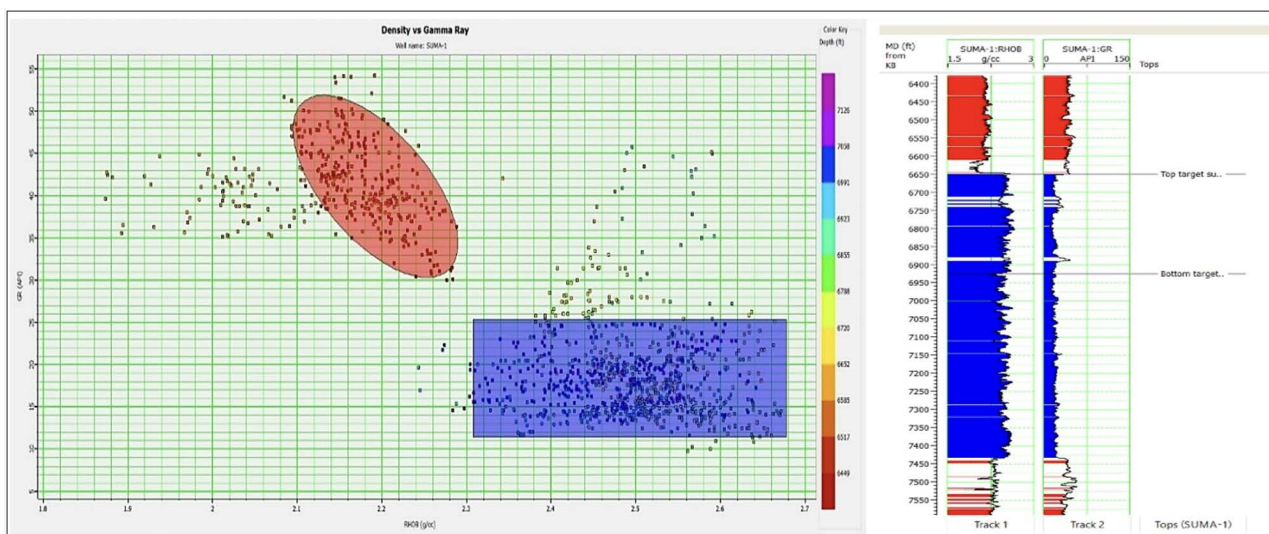


Figure 6. Crossplot of Gamma Ray log and RHOB log in Suma-1

crossover points to the presence of hydrocarbon fluids in the zone.

The acoustic impedance (AI) log (Figure 5f) is calculated by multiplying the sonic log (p-wave) velocity (Figure 5e) by the RHOB log. The acoustic impedance of a rock increases with its hardness and compactness (Agfa, 2018). Based on this, the reservoir target zone at a depth of 2,017-2,101 m, with a high AI value, is thought to be a layer of tight limestone lithology. The initial interpretation of the reservoir target zone indicates that it is a tight carbonate reservoir.

Sensitivity analysis

This analysis determines which parameters are most sensitive in distinguishing lithological distribution and reservoir characteristics within the target zone. This analysis entails generating crossplots from log data. This study creates a cross plot of the gamma-ray log and density porosity (RHOB) log using depth as the color key. The gamma ray and RHOB log crossplot (Figure 6) clearly separates the lithological distribution in the study. It has been observed that low gamma ray values correlate with high density values and vice versa. The

Table 1. Wavelet correlation

No	Wavelet	Wave Length	Max Correlation	Time Shift
1	Statistical	60	0.750	0
2	Statistical	100	0.867	0
3	Use Well	60	0.668	-1
4	Use Well	100	0.713	2

crossplot analysis classifies the lithological distribution into two formation zones: sandstone (red) and limestone/carbonate (blue). Sandstone Zone (red) is characterized by low density values (cutoff < 2.3 g/cc) and high gamma ray values (cutoff > 30 API). Limestone/Carbonate Zone (blue) has high density values (cutoff > 2.3 g/cc) and low gamma ray values (cutoff < 30 API).

The analysis results confirm the lithology log and gamma ray log interpretations, indicating that the target zone for the reservoir is in the limestone/carbonate lithology. The crossplot shows that sandstone or shale lithology has gamma ray values ranging from 30 to 55 API and density values of 1.9 to 2.3 g/cc. Limestone/carbonate lithology, on the other hand, has gamma ray values ranging from 10 to 30 API and density values of 2.3 to 2.68 g/cc.

Well-seismic tie

Before further processing or interpretation, the well seismic tie process must be completed between well and seismic data. This stage aims to bind or match the position of well log data in the time domain (two-way time) to seismic data in the depth domain using check-shots. Correlation can be performed after extracting the wavelet to produce a synthetic seismogram, which is then correlated with the well seismogram. The correlation process can be stopped when the correlation value is close to one and the time shift is 0 ms. Referring to Table 1, variations were made in this study by generating statistical and using well wavelets with wavelengths of 60 and 100,

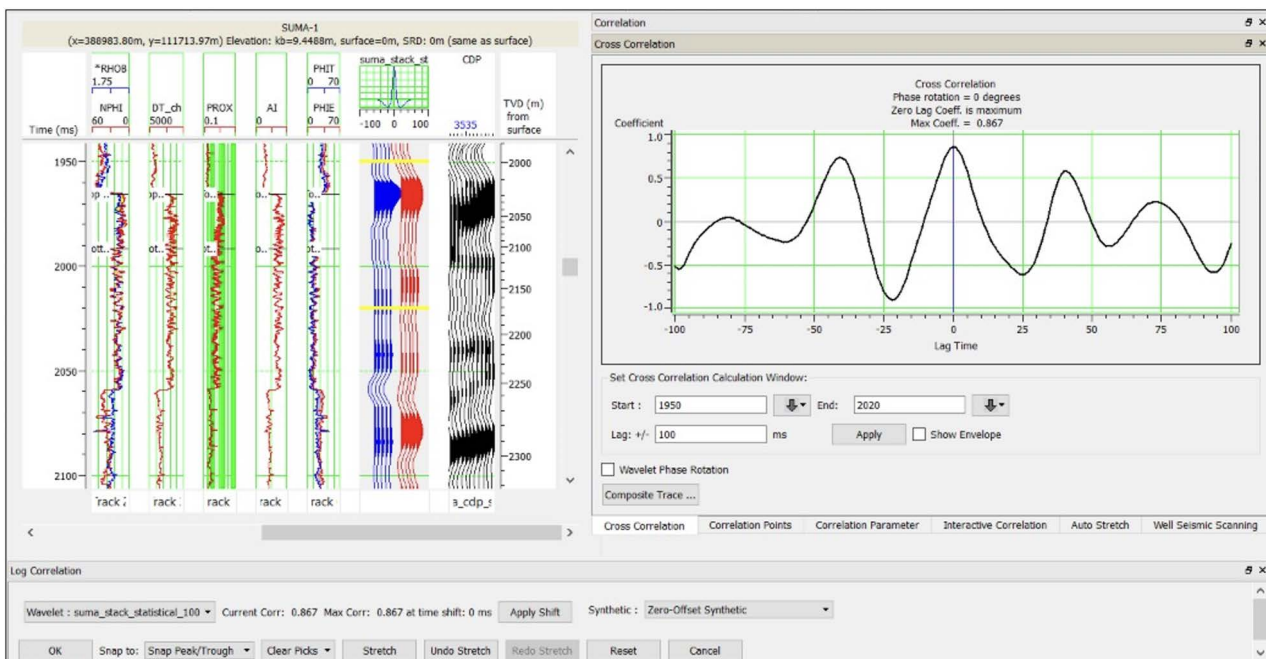


Figure 7. Well-to-seismic tie with statistical wavelet

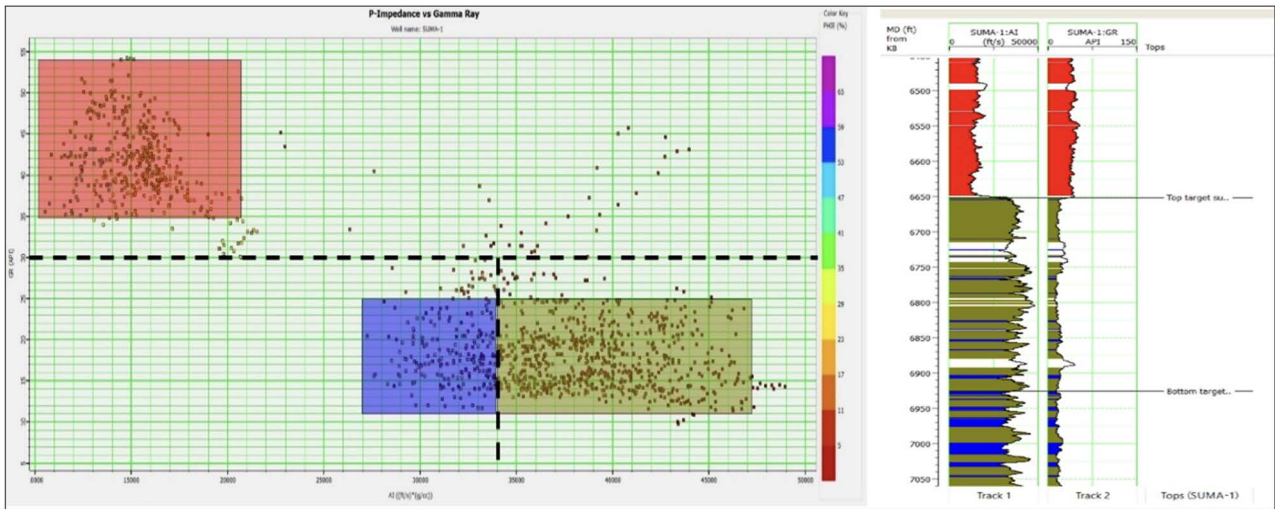


Figure 8. Crossplot of AI log and Gamma Ray log in Suma-1

respectively. During the well seismic tie process, a statistical wavelet was chosen to achieve the highest degree of similarity, with a correlation coefficient of 0.867 (Figure 7).

AI sensitivity analysis

AI sensitivity analysis verifies that other log parameters impact the AI log. This enables the AI log to distinguish between the distribution of rocks and

porosity value. Carbonate rocks (blue) have a relatively low AI value of 27,000 ft/s (g/cc), a relatively high porosity, and exhibit low gamma ray values (cutoff < 30 API). Carbonate rocks can be categorized into two main types: porous and tight. Porous carbonate rocks, represented in blue, have relatively low AI values ranging from 27,000 to 34,000 ft/s (g/cc) and exhibit higher porosity. In contrast, tight carbonate rocks, shown in green, have

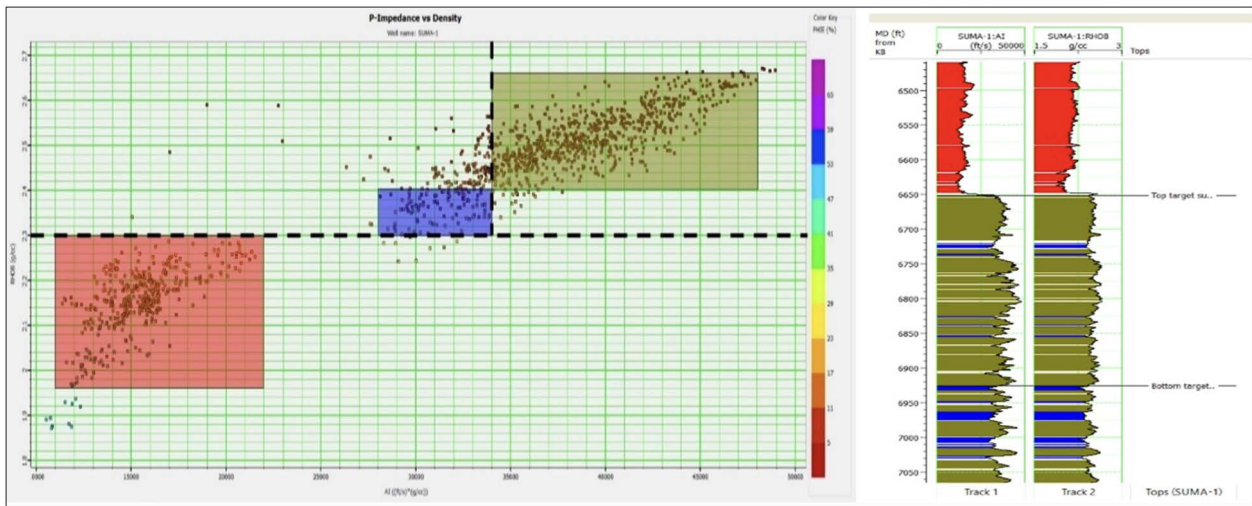


Figure 9. Crossplot of AI log and RHOB log in Suma-1

features in the reservoir or target zones. The AI sensitivity analysis in this study is done by plotting the AI log, the gamma-ray log, the RHOB log, and the NPHI log against the PHIE color key. The lithological distribution can be separated using a cross plot of the AI log and gamma-ray log in the Suma-1 well (Figure 8). The results show the distribution of sandstone (red) with higher gamma-ray values (cutoff > 30 API) and a relatively high

higher AI values exceeding 34,000 ft/s (g/cc) and lower porosity. The AI value of 34,000 (ft/s)(g/cc) serves as a cutoff or threshold to differentiate between these two types, as there is a significant difference in porosity.

As shown in Figure 9, the crossplot between the AI log and the RHOB log effectively separates the lithological distribution in the Suma-1 well. The crossplot analysis displays the distribution of

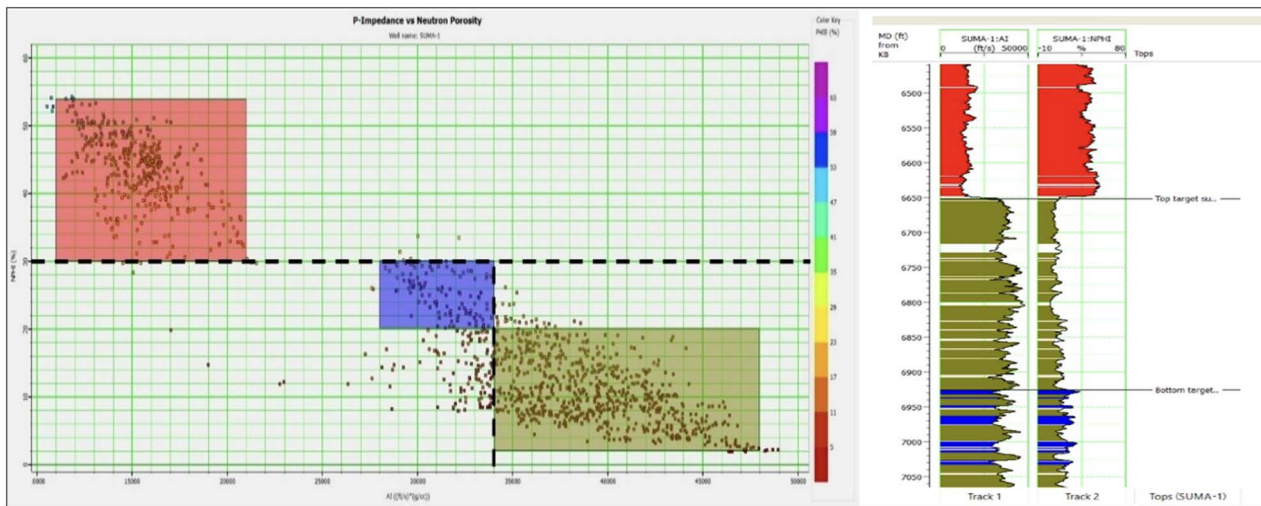


Figure 10. Crossplot of AI log and NPHI log in Suma-1

sandstones (red) with lower density values (cutoff < 2.3 g/cc), where the porosity values are relatively high. In contrast, carbonate rocks have higher density values (cutoff > 2.3 g/cc). Carbonate rocks are further divided into two categories: porous carbonate rocks and tight carbonate rocks. Porous carbonate rocks (blue) are characterized by relatively low AI values ranging from 28,000 to 34,000 (ft/s)(g/cc), along with relatively high porosity values. Tight carbonate rocks (green), on the other hand, have relatively high AI values > 34,000 (ft/s)(g/cc) and lower porosity values compared to porous carbonate rocks. The AI value of 34,000 (ft/s)*(g/cc) serves as a cutoff to distinguish between porous and tight carbonate rocks, as a clear difference in porosity values is observed at this point.

Figure 10 illustrates a crossplot between the AI log and the NPHI log that can separate the lithological distribution in the Suma-1 well. The results of the crossplot analysis show the distribution of sandstone (red) with a higher neutron porosity value (cutoff > 30%), where the porosity value is relatively high. Meanwhile, carbonate rocks have a low neutron porosity (cutoff < 30%). Carbonate rocks consist of porous carbonate rocks and tight carbonate rocks. Porous carbonate rocks (blue) are indicated by a relatively low AI value between 28,000 - 34,000 (ft/s)(g/cc), as well as a relatively high porosity value. Tight carbonate rocks (green) have a relatively high AI value > 34,000 (ft/s)(g/cc), with a relatively lower porosity value than porous carbonate rocks. The AI value of 34,000 (ft/s)*(g/cc) represents the boundary between porous and tight carbonate rocks.

The log data can be visualized as a cross-section. Different zones of sandstone lithology,

Table 2. Correlation coefficients and error values of six inversion methods

No	Inversion Method	Correlation	Error
1	<i>Model Based Hard Constraint</i>	0.997094	0.07937
2	<i>Model Based Soft Constraint</i>	0.995271	0.10424
3	<i>Bandlimited</i>	0.979209	-
4	<i>Colored Inversion</i>	0.923922	-
5	<i>Linear Programming Sparse Spike</i>	0.921927	0.41537
6	<i>Maximum Likelihood Sparse Spike</i>	0.956303	0.29658

porous carbonate, and tight carbonate are identified based on crossplot results. This cross-section effectively separates the target reservoir zone, a tight carbonate formation, from the surrounding sandstone and porous carbonate. These results confirm the initial interpretation from the AI log, indicating a tight carbonate reservoir. The crossplot analysis demonstrates that the acoustic impedance (AI), along with gamma ray, density, and neutron porosity logs, is highly effective in distinguishing the lithology of the target zone.

Pre-inversion analysis

Prior to performing seismic inversion, an initial model of the subsurface structure is created. Pre-inversion analysis then refines this model by selecting the most suitable inversion method and its parameters. This study employed various methods and parameters, aiming to achieve the highest correlation and lowest error between the inverted results (AI log and seismic trace) and the original well log and seismic data. Table 2 summarizes the correlation and error values for various inversion methods. As shown in the table, the model-based method with a hard constraint proved most effective, yielding the highest correlation (0.997094) and

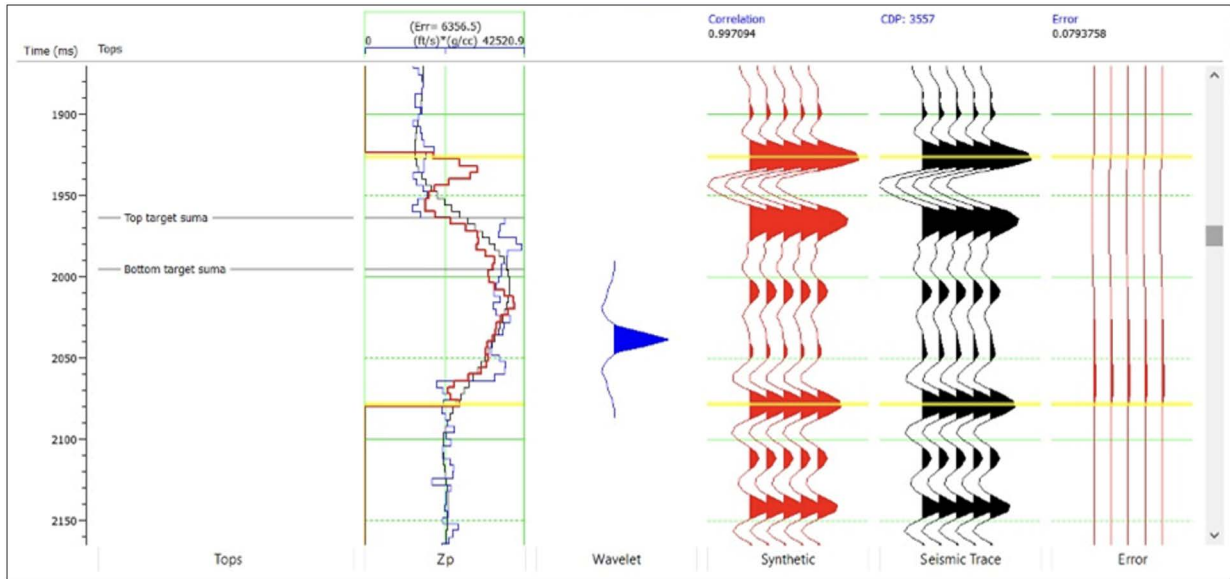


Figure 11. Pre-inversion analysis of model-based hard constraint

lowest error (0.07937) values among the tested methods.

A cross-section of the target reservoir zone using the model-based hard constraint inversion method was demonstrated on Figure 11. This cross-section allows for qualitative analysis of the relationship between the inverted AI log and synthetic seismic trace, compared to the original AI log and seismic trace. The deflection of the inverted AI log curve closely matches the original AI log, particularly in the high porosity zone. Additionally, the amplitude pattern of the synthetic seismic trace appears similar to that of the original seismic trace.

Figure 12 represents the acoustic impedance (AI) inversion results using the model-based hard constraint inversion. The inversion analysis reveals the distribution of lithology in the target reservoir zone and surrounding area. The lithologies mentioned include sandstone, porous, and tight carbonate rocks. The light blue purple coloured zone indicates that the target reservoir zone is at a depth of 1,963–1,995 m and has a high AI value, precisely 34,000–47,000 (ft/s) (g/cc). The target reservoir zone is presumed composed of tight carbonate rocks, specifically limestones from the Gomo Formation in the research area, which formed during the Middle Miocene-Early Pliocene era.

AI Inversion

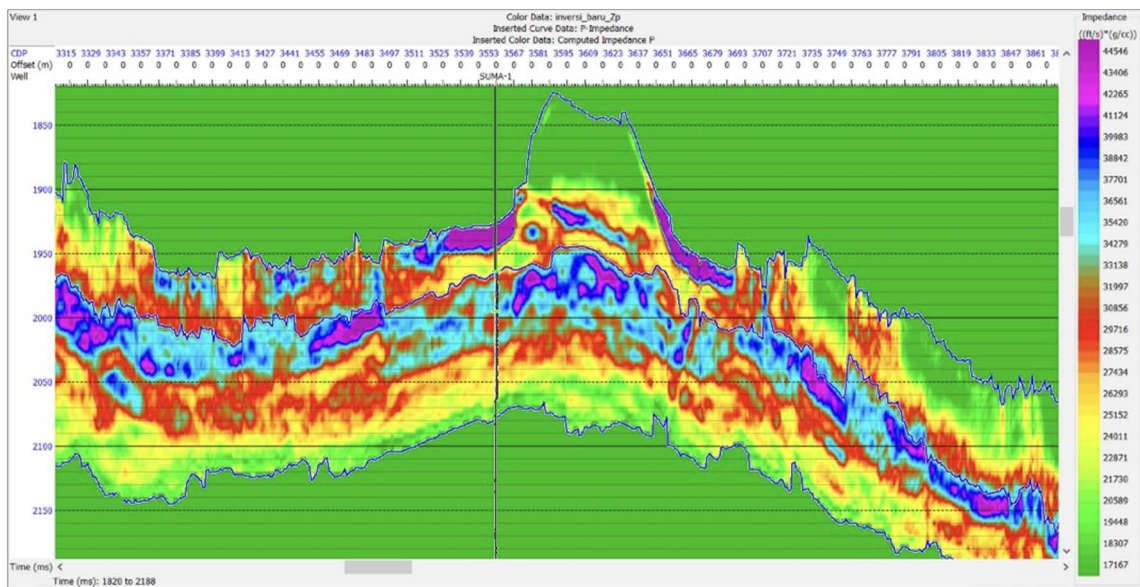


Figure 12. AI Inversion model

The orange-red colored zone indicates the distribution of porous carbonate rocks from the same formation, which have a moderate AI value ranging from 27,000 to 34,000 (ft/s)(g/cc). Furthermore, the distribution of sandstone in the inversion cross-section has a low AI value ranging from 11,000 to 21,000 (ft/s)*(g/cc) in the green-yellow colored zone. The AI inversion results shown are consistent with the log crossplot results between the gamma ray and AI logs.

DISCUSSIONS

Using 2D forward modelling on the residual gravity anomaly along the same section as the seismic line (Figure 13) brings together the

the generated model closely resembles the actual subsurface geological conditions of the Nias Basin.

The forward modelling results significantly correlate with the seismic amplitude cross-section shown in Figure 14. The seismic data that has been interpreted (yellow, green, and blue lines) shows a structure that closely resembles the one predicted through forward modelling. In ideal oil and gas basins, these structural configurations serve as natural traps, capturing migrating hydrocarbon fluids.

Analysis of well log data (e.g., gamma-ray log) from the Suma-1 well places the target reservoir zone at approximately 2017 m to 2101 m depth. The well-log interpretation shows that the zone is part of the Gomo Formation, formed in the research area between the

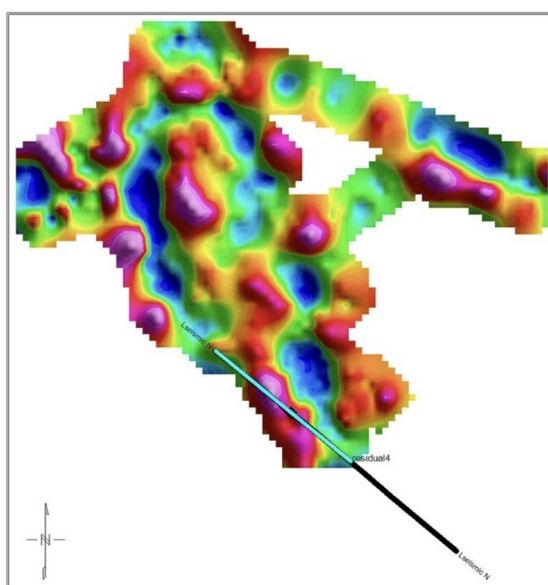


Figure 13. Cross-sectional from residual anomaly aligned with seismic lines

processing of gravity data and the analysis of seismic data. The figure displays the seismic survey line (black) and the 2D forward modeling section (light blue line). Because a portion of the seismic line falls outside the available gravity data coverage (as shown on the map), forward modeling was only applied to roughly half of the seismic line's length.

Forward modelling along the same geological profile as the seismic line produces similar to modelling gravity data in other sections. According to Figure 14, the model depicts a high structure in the middle of the line, with basins on the western and eastern sides. Notably, the cross-section model yields a remarkably low error value of 0.176%, well within the acceptable range. This accomplishment indicates that

Middle Miocene and Early Pliocene. However, the forward modelling results suggest that the target zone may be in the upper Lelematua Formation. This difference could be due to the uncertainties associated with forward modelling techniques.

In addition, the upper Lelematua Formation exhibits a finger-like interfingering structure with the lower Gomo Formation, potentially causing unclear formation boundaries within the target zone. This complexity can contribute to challenges in both interpretation and forward modeling. Consequently, the results of the gravity method need to be checked and confirmed by collecting more seismic data and using gravity-seismic joint inversion.

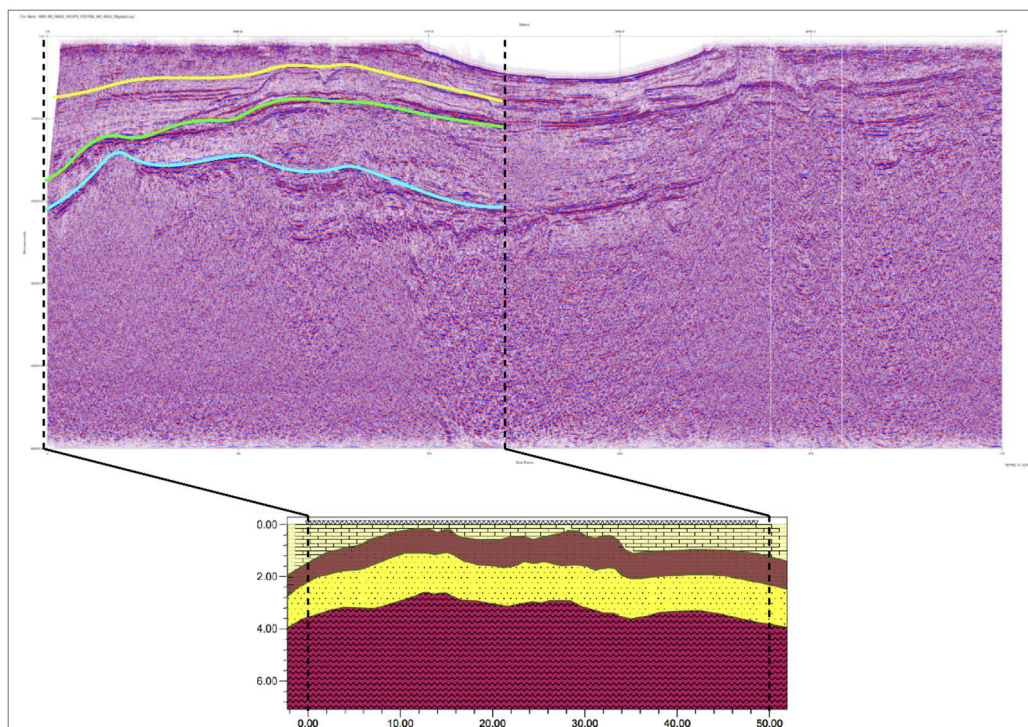


Figure 14. Correlation of forward modeling with seismic amplitude cross-section

CONCLUSIONS

The residual gravity anomaly reveals 8 sub-basin patterns distributed in the research area. These patterns follow the lineaments of the Nias Basin's basement highs and are thought to be connected in a northwest-southeast direction.

Four rock formations were identified based on the subsurface geological model constructed using 2D forward modeling. The deepest layer is metamorphic bedrock, with a density of 2.7 g/cc. The Gomo Formation, which has a density of 2.4 g/cc, follows the Lelematua Formation beneath this. The Gunungsitoli Formation caps the sequence. The uppermost layer is alluvium, with a density of 2.25 g/cc. The model-based hard constraint inversion method was used on the Suma-1 well in the Nias Basin, and the results are promising for exploring for hydrocarbons. The analysis suggests the potential hydrocarbon accumulations at a depth of 2,017-2,101 m. Based on sensitivity analysis with an interval of 34,000 - 47,000 (ft/s)*(g/cc), an AI cutoff value of more than 34,000 (ft/s)*(g/cc) was obtained. The carbonate is estimated to be a tight carbonate of the Gomo Formation limestones.

ACKNOWLEDGEMENTS

The authors wish to thank the Marine Geological Institute for providing access to data

sources for this study. We acknowledge the help of all the 2017 Nias Biogenic Gas Team and RV Geomarin 3 crew in acquiring the marine gravity and 2D seismic data. Thanks also directed to faculty members of the Geophysics Department of ITS for the discussions during this research.

REFERENCES

- Agfa, C. I., 2018. *Aplikasi Metode Inversi Impedansi Akustik dan Seismik Multiatribut Untuk Karakteristik Zona Reservoir Hidrokarbon Pada Lapangan "CVN" Cekungan Sumatera Tengah*, Undergraduate thesis, Institut Teknologi Sepuluh Nopember Surabaya, p.14.
- Alifudin, R. F., Lestari, W., Syaifuddin, F. and Haidar M. W., 2016. Karakterisasi Reservoir Karbonat Dengan Aplikasi Seismik Atribut Dan Inversi Seismik Impedansi Akustik. *Jurnal Geosaintek*, 2(2):107-112
- Djamal, B., Gunawan, W., Simanjuntak, T.O., and Ratman, N., 1994. *Geological Map of The Nias Quadrangle, Sumatra*, Pusat Penelitian dan Pengembangan Geologi, Bandung.
- Deighton, I., Mukti, M.M., Singh, S.C., Travis, T.C., Hardwick, A., and Herson, K., 2014. Nias Basin, NW Sumatra – New Insights into Forearc Structure and Hydrocarbon

- Prospectivity from Long-Offset 2d Seismic Data. *Proceedings, Indonesian Petroleum Association, Thirty-Eight Annual Convention & Exhibition, May 2014, IPA14-G-299.*
- Dewi, I. K., Puspitasari, F., Nasri, M. Z., and Martha, A., 2020. Pemodelan 3D Data Gravity Untuk Identifikasi Struktur Pembentukan Cekungan Hidrokarbon Wilayah Bajubang Provinsi Jambi. *Jurnal Geofisika Eksplorasi* 6(3): 216-227. <https://doi.org/10.23960/jge.v6i3.10>
- El-Sehamy, M., Abdel Gawad, A. M., Aggour, T. A., Orabi, A. H., Abdella, H. F., and Eldosouky, A. M., 2022. Sedimentary cover determination and structural architecture from gravity data: East of Suez Area, Sinai, Egypt. *Arabian Journal of Geosciences*, 15 (109). doi:10.1007/s12517-021-09348-6
- Erviantari, D. and Sarkowi, M., 2014. Studi Identifikasi Struktur Bawah Permukaan Dan Keberadaan Hidrokarbon Berdasarkan Data Anomali Gayaberat Pada Daerah Cekungan Kalimantan Tengah. *Jurnal Geofisika Eksplorasi*, 2(1): 13-20
- Karig, D. E., G. F. Moore, Curray J. R., and Lawrence M. B., 1980, Morphology and shallow structure of the lower trench slope off Nias Island, Sunda Arc, in D. E. Hayes (ed.) *The Tectonic and Geologic Evolution of Southeast Asian Seas and Islands, AGU Monograph*, 23; 179-208
- Lghoul, M., Abd-Elhamid, H.F., Zelenáková, M., Abdelrahman, K., Fnais, M.S., and Sbihi, K., 2023. Application of enhanced methods of gravity data analysis for mapping the subsurface structure of the bahira basin in Morocco. *Frontier in Earth Science*. 11:1225714. <https://doi.org/10.3389/feart.2023.1225714>
- Nzeuga, A. R., Ghomeshi, F., Pham, L. T., Eldosouky, A. M., Aretouyap, Z., Kana, J. D., et al., 2022. Contribution of advanced edge-detection methods of potential field data in the tectonic-structural study of the southwestern part of Cameroon. *Front. Earth Sci.* 10: 1–15. <https://doi.org/10.3389/feart.2022.970614>
- Permana, H., Handayani, L. and Gaffar, E. Z., 2010. Studi Awal Pola Struktur Busur Muka Aceh, Sumatera Bagian Utara (Indonesia): Penafsiran dan Analisa Peta Batimetri. *Jurnal Geologi Kelautan*, 8(3): 105-118
- Pham, L. T., Ghomsi, F. E., Vu, T. V., Oksum, E., Steffen, R., and Tenzer, R., 2023. Mapping the structural configuration of the Western Gulf of Guinea using advanced gravity interpretation methods. *Physics and Chemistry of the Earth, Part A/B/C*. 129: 103341. <https://doi.org/10.1016/j.pce.2022.103341>
- Pradana, D. R., Lestari, W. & Syaifuddin, F., 2017. Analisis Sebaran Litologi Batu Pasir Dakota Menggunakan Metode Seismik Inversi Berbasis Model, Studi Kasus Lapangan Teapot, Wyoming, USA. *Jurnal Sains Dan Seni POMITS*, 6(2): 25-28
- Prastika, N., Sapto, B., Dewanto, O., and Wijaksono, E., 2018. Analisis Perbandingan Metode Seismik Inversi Impedansi Akustik Model Based, Band Limited, Dan Sparse Spike Untuk Karakterisasi Reservoir Karbonat Lapangan "NBL" Pada Cekungan Nias. *Jurnal Geofisika Eksplorasi*, 2(17)
- Rahardiawan, R., 2018. *Laporan Akhir Penelitian Gas Biogenik Cekungan Nias, Sumatera Utara (Survei KR Geomarin III)*. Pusat Penelitian dan Pengembangan Geologi Kelautan, Kementerian Energi dan Sumber Daya Mineral. Internal report. Unpublished.
- Rose, R., 1983, Miocene carbonate rocks of Sibolga Basin, northwest Sumatra: 12th *Indonesian Petroleum Association Annual Convention*: 107-125
- Saada, S. A., Eldosouky, A. M., Kamel, M., El Khadragy, A., Abdelrahman, K., and Fnais, M. S., 2022. Understanding the structural framework controlling the sedimentary basins from the integration of gravity and magnetic data: A case study from the east of the qattara depression area. *Egypt. Journal of King Saud University-Science*. 34: 101808. <https://doi.org/10.1016/j.jksus.2021.101808>
- Sapiie, B., 2015. Geology and Tectonic Evolution of Fore-arc Basin: Implications of Future Hydrocarbon Potential in The Western Indonesia. *Proceedings Indonesian Petroleum Association, Thirty-Ninth Annual Convention & Exhibition*. IPA15-G-117
- Setiadi, I., Diyanti, A. dan Ardi, N.D., 2014. Interpretasi Struktur Geologi Bawah

- Permukaan Daerah Leuwidamar Berdasarkan Analisis Spektral Data Gaya Berat, *Jurnal Geologi dan Sumber Daya Mineral*, 15(4): pp. 205–214, 2014
- Setiadi, I., Purwanto, C., Kusnida, D., dan Firdaus, Y., 2019. Interpretasi Geologi Berdasarkan Analisis Data Gaya berat Menggunakan Filter Optimum Upward Continuation Dan Pemodelan 3D Inversi (Studi Kasus Cekungan Akimeugah Selatan Laut Arafura). *Jurnal Geologi Kelautan*, 17(1): 33-48
- Talwani, M., Worzel, J.L. and Landisman, M., 1959. Rapid Gravity Computations for Two-Dimensional Bodies with Application to the Mendocino Submarine Fracture Zone. *Journal of Geophysical Research*, 64: 49-59.
- Telford, W.M., Geldart, L.P., and Sheriff, R.E., 1990. *Applied Geophysics* (2nd edition). Cambridge University Press.